
Proceedings Paper:
Njobuenwu, DO and Fairweather, M (2015) Preferential Concentration of Inertial Fibres in a Turbulent Channel Flow. In: Simos, TE, Kalogiratou, K and Monovasilis, T, (eds.) AIP Conf. Proc. 1702. International Conference of Computational Methods in Sciences and Engineering 2015 (ICCMSE 2015), 20-23 Mar 2015, Athens, Greece. American Institute of Physics , 080009-080009. ISBN 978-0-7354-1349-8

https://doi.org/10.1063/1.4938804

Preferential Concentration of Inertial Fibres in a Turbulent Channel Flow

D.O. Njobuenwu and M. Fairweather

Institute of Particle Science and Engineering, School of Chemical and Process Engineering, University of Leeds, Leeds LS2 9JT, UK
D.O.Njobuenwu@leeds.ac.uk

Abstract. Large eddy simulation (LES) is developed to study particle preferential concentration, in which an initially uniform distribution of inertial particles spontaneously segregates into clusters in a turbulent flow, driven primarily by the small-scale turbulent fluctuations and slip velocity. Dynamic modelling of sub-grid scale effects on the LES and Langevin-type sub-grid scale modelling of particle motion ensures particle clustering is well captured, which is computational cheap when compared to fully-resolved simulations. Results shows that prediction of particle clustering near walls due to turbophoresis is strongly depended on (i) the particle inertia, where particle inertia is parameterised by its Stokes number, (ii) particle shape, parameterised by its aspect ratio, (iii) binning method and (iv) simulation time.

Keywords: **Large eddy simulation, Ellipsoids, Orientation, Preferential concentration, Channel flow, Turbulence.**
PACS: 45.20.dc, 87.15.hj, 45.40.Bb, 45.40.-f, 47.55.Kf

INTRODUCTION

The transport of fibrous, rod- or needle-like particles in turbulent flows has many industrial, environmental and biomedical applications. In most of these, it is important to understand particle dispersion, agglomeration and deposition on any rigid boundary, and re-suspension into the core flow due to turbulence and inertia, as well as to obtain a quantitative measure of the tendency of these phenomena to occur. Of interest in this work is the influence of flow turbulence, particle inertia and particle shape and orientation on its dispersion leading to preferential concentration. Preferential concentration, often called turbophoresis, refers to the strong inhomogeneities in the spatial distribution of particles suspended in a turbulent flow. The intensity of the relative velocity between a particle and the fluid produces various anomalous phenomena such as small-scale clustering or preferential accumulation at the wall for bounded and unbounded turbulent flows [1, 2]. Regions of either high or low particle concentration may be associated with specific turbulent structures, or may be formed by the action of turbulent eddies over a short time preceding the observation. In situations where physical, chemical or biological interaction between particles is required, such inhomogeneities affect the probability of finding particles close to one another which influences their collision probability, or biological, chemical or gravitational interaction. This phenomena is still not understood for non-spherical and even spherical particles; there is therefore a need to further study the nature and dynamics of these inhomogeneities and their association with fluid turbulence structures [3].

Direct numerical simulations (DNS) of particle-laden turbulent flows capture all the relevant energetic scales and are therefore able to correctly predict preferential concentration [3], but are limited to low Reynolds number flows. Reynolds-averaged Navier-Stokes techniques model the average turbulent velocity field, with dispersion models to account for the effect of turbulent fluctuations on particle motion, but contain none of the physics responsible for particle preferential concentration. Large eddy simulation (LES) captures the large and models the small (sub-grid) energetic scales, and with appropriate sub-grid scale (SGS) models and SGS modelling of inertial particle motion can recover the preferential concentration of inertial particles.

In this work, the preferential concentration of fibrous particles, analogous to prolate spheroids with aspect ratio $\lambda > 1$, in a fully developed channel flow at low shear Reynolds number $Re_\tau = 150$ is studied. The approach uses LES

with a dynamic sub-grid scale model for the flow while the dynamics of the particles is obtained from solution of the linear and angular momenta in a Lagrangian framework. To address the challenge of particle drag coefficients for particles with finite particle Reynolds number Re_p >>1 which are beyond the Stokesian regime, we use the Ganser [4] empirical drag correlations, developed for high Re_p. In the model, we use the equivalent diameter d_{eq} as the geometric parameter, and the aspect ratio λ and sphericity Φ_s as shape factors in the empirical drag coefficient, C_D, to account for the departure in shape from spherical, and model the dependence of the particle dynamic orientation by using the projected area A_D. The particle dynamic projected area is expressed by a functional relationship of the dynamic incidence angle α_i, and the particle dimension using the particle semi-minor axis a and aspect ratio $\lambda=c/a$. This method has been applied previously to model the motion of non-spherical particles, including cylinders in laminar flows [5], and spheres, needles and disks in turbulent flows [6]. The governing equations for the continuous phase, as well as the translation equations for fibres, are in the inertial co-ordinate frame, while rotational equations for ellipsoidal particles are in a particle frame. The transformation between the inertial and the particle frames is expressed as $\mathbf{x'}=\mathbf{A.x}$, where $\mathbf{A}=[a_{ij}]$ is the time-dependent rotational matrix, and its elements a_{ij} can be expressed in terms of four Euler quaternions.

The drag force and profile lift force due to the particle orientation acting on a single particle are expressed as [7]:

$$\mathbf{F_D} = \tfrac{1}{2}\rho A_D C_D \,|\mathbf{u}-\mathbf{v}|\,(\mathbf{u}-\mathbf{v}), \tag{1}$$

$$\mathbf{F_{PL}} = \tfrac{1}{2}\rho A_L C_L \frac{\mathbf{z'}.(\mathbf{u}-\mathbf{v})}{|\mathbf{u}-\mathbf{v}|}\left[\mathbf{z'}\times(\mathbf{u}-\mathbf{v})\right]\times(\mathbf{u}-\mathbf{v}), \tag{2}$$

where $\mathbf{u}=[u_x,u_y,u_z]$ and $\mathbf{v}=[v_x,v_y,v_z]$ are the fluid and particle velocity vectors at the particle centroid, $\mathbf{z'}$ is the direction of the particle major axis, and A_D and A_L are the particle projected areas normal to the direction of the drag and profile lift forces, respectively. Using the Markov assumption for the velocity of a stochastic particle in a turbulent flow field, a generalised Langevin stochastic differential equation formulated as a function of the SGS kinetic energy and particle relaxation time was used to model the effect of SGS velocity fluctuations on the particle acceleration [8]. The rotation of the particle is given by the Euler rotational equation as:

$$\mathbf{I}\cdot\frac{\mathrm{d}\boldsymbol{\Omega}'(t)}{\mathrm{d}t} = \mathbf{T}(t)+\boldsymbol{\Omega}'(t)\times[\mathbf{I}\cdot\boldsymbol{\Omega}'(t)], \tag{3}$$

where $\mathbf{I}$ is the inertia tensor, $\boldsymbol{\Omega}'=[\Omega_{x'},\Omega_{y'},\Omega_{z'}]$ is the angular velocity, and $\mathbf{T}=\mathbf{T_1}+\mathbf{T_2}$ is the net torque exerted on the particle caused by the non-coincident centres of mass and of pressure, $\mathbf{T_1}$, and the torque due to the resistance on a relatively rotating body, $\mathbf{T_2}$, which always acts to attenuate the relative rotation [5]. The rate of change of the fibre position is given as $\mathrm{d}\mathbf{x_p}/\mathrm{d}t=\mathbf{v}$ and the orientation $\dot{\mathbf{q}}$ due to the angular velocity in the particle frame is given as:

$$\frac{\mathrm{d}\mathbf{q}}{\mathrm{d}t} = \begin{pmatrix}\dot{q}_0\\ \dot{q}_1\\ \dot{q}_2\\ \dot{q}_3\end{pmatrix} = \frac{1}{2}\begin{bmatrix} q_o & -q_1 & -q_2 & -q_3\\ q_1 & q_0 & -q_3 & q_2\\ q_2 & q_3 & q_0 & -q_1\\ q_3 & -q_2 & q_1 & q_0\end{bmatrix}\begin{bmatrix}0\\ \Omega_{x'}\\ \Omega_{y'}\\ \Omega_{z'}\end{bmatrix}. \tag{4}$$

A 4th order Runge-Kutta algorithm was used to solve the equations of motion to obtain the particle position, velocity, rotation and orientation with time. Fluid properties at the particle position were obtained using sixth-order Lagrangian polynomials. The particles were randomly seeded in the domain whilst their initial orientation was randomly imposed with the three Euler angles, while the linear and angular velocity components were set equal to those of the fluid at the particle position. Large eddy simulation with a dynamic sub-grid scale model was used to solve the continuity and Navier-Stokes equations that govern the Eulerian fluid dynamics. BOFFIN, a finite-volume code, which is based on a fully implicit low-Mach number formulation and is second-order accurate in both space and time, was used to solve the governing equations [8]. The computational domain was a channel flow with size ($2h\times2h\pi\times2h\pi$), which was discretised in physical space with 129×128×128 grid points with a uniform mesh along the homogenous directions and a smoothly varying mesh based on hyperbolic functions along the x-axis. The Reynolds number $Re_\tau = hu_\tau/\nu$ was 150, with other parameters identical to those of [3]. Periodic boundary conditions were applied in the homogeneous directions for both the fluid and particle phases, while perfect elastic collision was adopted for particle-wall interactions.

RESULTS AND DISCUSSION

The time- and spaced-averaged first and second statistical moments of the fluid and the particles, though not shown here in the interests of brevity, were in good agreement [6] with those reported in [3]. The particle concentration was computed by averaging the number of particles over the i^{th} wall-parallel bin along the wall-normal direction, with (A) the same thicknesses $\Delta x^+(i)$ as the control volumes used for discretisation in the LES, and (B) the thickness of the i^{th} bin, $\Delta x^+(i)$, obtained by means of hyperbolic tangent binning, as used in [3].

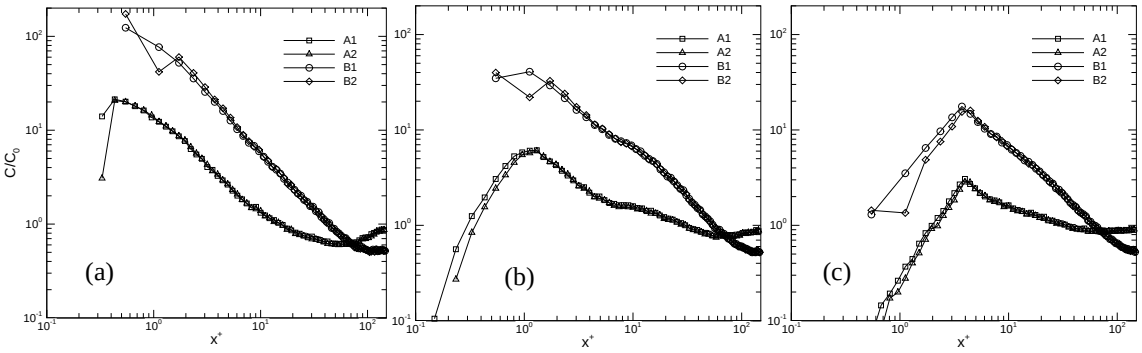

FIGURE 1. Instantaneous particle number density wall-normal profiles for dimensionless particle equivalent relaxation time (Stokes number) τ^+_{ev} =15 with different binning methods and particle shapes (aspect ratios) λ = (a) 1, (b) 10 and (c) 50.

Following the method of Marchioli et al. [3], particle concentration was obtained as follows: (i) the flow domain was divided into bins according to the aforementioned binning procedures (A) and (B); (ii) at any instant in time the number of particles within each bin was determined following two methods: (1) counting the particles in the index i cell associated with the lower face of the host cell (i.e. the cell containing the particle), and (2) counting the particles in the index i cell plus the ratio, x_R, of the wall-normal particle position within the host cell to the host cell height; (iii) dividing the number of particles obtained in (ii) by the volume of that bin to obtain the local concentration, $C=C(i)$; (iv) normalise C with its initial value C_0 to obtain C/C_0, the particle number density distribution, with $C/C_0 \approx 1$ representing a uniform distribution, $C/C_0 >> 1$ flow regions where particles preferentially distribute and $C/C_0 < 1$ flow regions depleted of particles. Based on these binning procedures, results are considered in terms of the effect of binning method (A1, A2, B1 and B2), particle shape (λ=1, 1.001, 3, 10, 30 and 50) and particle inertia (τ^+_{ev}=1, 5, 15, 25, 50 and 100) on particle clustering and segregation near the wall due to turbophoresis.

The particle concentration profiles are shown in Figs. 1 and 2. Very high particle concentrations near the wall can generally be observed for all cases, indicating that the method adopted is able to capture the effects of turbophoresis. The technique developed here is computationally inexpensive, and accurate in comparison to fully-resolved simulations for τ^+_{ev}=1, 5 and 25 for spherical particles with λ=1 [3]. Under-prediction of the latter results in the present case is most likely due to the fact that the LES results in the near-wall region are still developing, whilst the benchmark DNS results [3] were computed when the particle distribution had reached steady-state. Even in the five DNS results reported in [3], however, there were differences between the predictions of different DNS codes. As noted in [3], the reasons for these differences include, amongst others, the use of different numerical schemes and grid discretisations in each case, and numerical errors associated with different interpolation techniques and the choice of the time-step used to integrate the equation of motion for the particles. These numerical errors sum up over time, and give the accumulated profile deviations observed between each set of predictions.

Particle concentration is higher in the near-wall region than in the core flow and remains uniform only for a small area close to the channel centre line for all the particle inertia and shapes considered. The small concentration of particles in the core region demonstrates that in order to get accurate results, the number of particles must be large. Results of the concentration are sensitive to the method of binning and bin size, with the B2, B1, A2 and A1 methods showing the largest values in that order. In terms of shape, the spherical particles (λ=1 and 1.001) show the highest concentration in the near-wall region, whilst the most elongated particles show the lowest near-wall concentration. Preferential concentration increases from τ^+_{ev}=1 and peaks at τ^+_{ev}=15, gradually reducing with further increases in τ^+_{ev}.

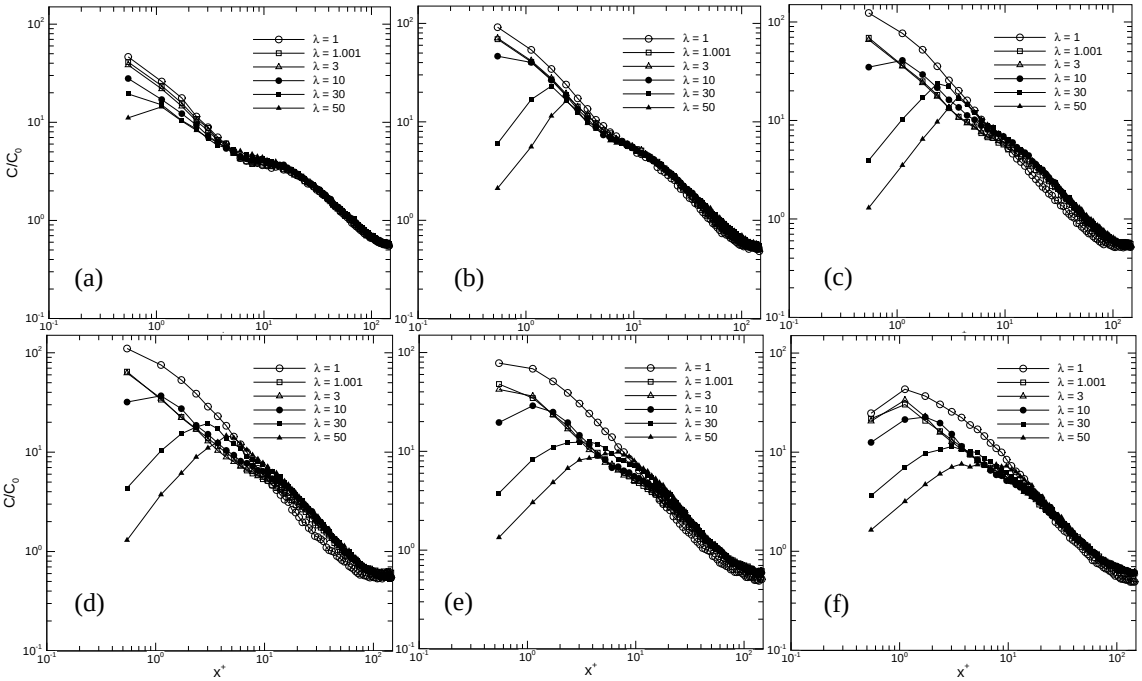

FIGURE 2. Instantaneous particle number density wall-normal profiles for binning method B1 and for dimensionless particle equivalent relaxation time (Stokes number) τ^{+}_{ev} = (a) 1, (b) 5, (c) 15, (d) 25, (e) 50 and (f) 100.

CONCLUSIONS

A number of simulations for inertial particles with varying aspect ratio were carried out to study the effect of binning methods, particle shape and inertia on particle clustering and segregation near a channel wall due to turbophoresis. Turbophoresis occurred for all particle sizes and shapes considered. With respect to the binning procedure, the value of C/C_0 is highest in the following order: B2, B1, A2 and A1, with the former values larger than the latter since the bin size closest to the wall for B1 and B2 is of the order of the particle diameter for τ^{+}_{ev}=25. Values of C/C_0 obtained from method (2), noted above, are also larger than those from method (1). In terms of shape, the spherical particles show the highest concentration in the near-wall region, whilst the most elongated particles show the lowest near-wall concentration.

ACKNOWLEDGMENTS

The authors wish to thank the Engineering and Physical Sciences Research Council for their financial support of the work reported in this paper under EPSRC Grant EP/I003010/1.

REFERENCES

1. M.W. Reeks, *J. Aerosol. Sci.* **14**, 729-739 (1983).
2. G. Sardina, F. Picano, P. Schlatter, L. Brandt and C. Casciola, *Flow Turbul. Combust.* **86**, 519-532 (2011).
3. C. Marchioli, A. Soldati, J.G.M. Kuerten, B. Arcen, A. Tanière, G. Goldensoph, K.D. Squires, M.F. Cargnelutti and L.M. Portela, *Int. J. Multiphas. Flow* **34**, 879-893 (2008).
4. G.H. Ganser, *Powder Technol.* **77**, 143-152 (1993).
5. C. Yin, L. Rosendahl, S.K. Kær and H. Sørensen, *Chem. Eng. Sci.* **58**, 3489-3498 (2003).
6. D. O. Njobuenwu and M. Fairweather, *Chem. Eng. Sci.* **123**, 265-282 (2015).
7. H. Brenner, *Chem. Eng. Sci.* **19**, 703-727 (1964).
8. M. Bini and W. P. Jones, *J. Fluid Mech.* **614**, 207-252 (2008).